

Nucleon-antinucleon resonance spectrum in a potential model

M. Lacombe* and B. Loiseau

*Division de Physique Théorique, Institut de Physique Nucléaire, 91406 Orsay, France
and Laboratoire de Physique Théorique des Particules Élémentaires,
Université Pierre et Marie Curie, Paris 75230 Cedex 05, France*

B. Moussallam and R. Vinh Mau

*Physics Department, State University of New York at Stony Brook, Stony Brook, New York 11794
and Division de Physique Théorique, Institut de Physique Nucléaire, 91406, Orsay, France*

(Received 28 December 1983)

We investigate the spectrum of antinucleon-nucleon resonances, using an optical potential we derived recently. An effective method to compute the S -matrix poles is presented. The corresponding phase shifts do not behave as ordinary resonances in the Argand diagram. We show, however, that the poles can be located by extrapolating the phase shifts with the aid of polynomial fits. The annihilation part of our potential is state and energy dependent and of short range. It yields a richer spectrum than that given by a longer ranged annihilation model.

I. INTRODUCTION

The existence of an exotic class of mesons with a strong coupling to the $N\bar{N}$ system has been discussed during the last few years. A number of candidates have been proposed by experimentalists. They are not, however, confirmed by more recent experiments.¹ Progress and clarification are expected, very soon, from the low energy antiproton ring (LEAR) facility.²

The description of these mesons in terms of quarks with a possible $2q2\bar{q}$ structure has been considered by various authors.³ They can also be viewed as bound states or resonances produced by an optical potential. This picture is called the quasinuclear model.⁴ We do not know how to reconcile these different approaches, but it seems plausible that those states which lie in the vicinity of the $N\bar{N}$ threshold will contain a large $N\bar{N}$ admixture in their wave functions. The situation is reminiscent of that of the scalar 0^{++} mesons $S(980)$, $\delta(980)$, and $\epsilon(1300)$. Recent studies tend to indicate that they are actually closer to resonant combinations of two mesons than to $q\bar{q}$ or $2q2\bar{q}$ bags.⁵ In any event, it appears quite important to have definite predictions from the quasinuclear model.

The quasinuclear model is based on the fact that the real part of the $N\bar{N}$ optical potential due to meson exchanges is much more attractive than the corresponding NN potential, giving rise to a rich spectrum of discrete states. The imaginary part of the potential, due to annihilation, gives widths to these states. Predictions on the widths vary with the assumed potential. For instance, the Argand diagrams for the Bryan-Phillips potential do not show any resonance effect in the usual sense.⁶ Later work, on the contrary, indicates that the $N\bar{N}$ S matrix could possess poles close to the real axis.^{7,8}

Recently, we constructed a $N\bar{N}$ optical potential, the long and medium range parts of which are the G -parity transform of the Paris NN potential. The annihilation part is energy and state dependent, and of short range as

suggested qualitatively by a calculation of simple annihilation box diagrams. This potential,⁹ which will be referred to, hereafter, as the Paris $N\bar{N}$ potential, yields a very good fit to the existing low energy $p\bar{p}$ scattering data. The main purpose of the present work is to study the spectrum of resonances predicted by this model.

We proceed as follows. In Sec. II, we describe the procedure to search for the S -matrix poles. We first derive a direct method to calculate the complex zeros of the Jost function. Then, we show that these results can be recovered by using suitable polynomial approximations of the inverse S matrix over the physical domain. This provides a link between the scattering data and the poles. In Sec. III, we apply these methods to the Paris $N\bar{N}$ potential and, in order to get some insight into the dependence on the model, especially the properties of the annihilation part, to the Dover-Richard potential.¹⁰ The latter has a local and central annihilation part of somewhat longer range. The spectrum from the Paris potential displays more resonant structure than the latter. Relevant formulae to calculate the Jost function are collected in the Appendix.

II. SEARCH PROCEDURE FOR THE S -MATRIX POLES

A. Direct method: Zeros of the Jost function in the complex momentum plane

Let us recall that, in potential scattering, for a particular partial wave, the S matrix can be written in terms of the Jost function as¹¹

$$S(k) = \frac{F(-k)}{F(k)}, \quad (2.1)$$

with

$$k^2 = Em = \frac{mT_L}{2}; \quad (2.2)$$

m is the nucleon mass, E is the c.m. relative energy, and T_L is the laboratory kinetic energy.

If the potential consists of a superposition of Yukawa terms, as here, then $F(k)$ is analytic in the complex k plane with a cut along the imaginary axis. This cut, for NN or $N\bar{N}$ scattering, corresponds to $-\infty < \text{Im}k < -(m_\pi/2)$, where m_π is the pion mass ($m_\pi \sim 0.7 \text{ fm}^{-1}$). Resonances correspond to the zeros of $F(k)$ in the domain $\text{Im}k < 0, \text{Re}k > 0$. The usual way to compute $F(k)$ is to form the Wronskian of the regular solution of the Schrödinger equation with the outgoing free solution at large enough r . It turns out, unfortunately, that the limit $r \rightarrow \infty$ does not exist if $\text{Im}k < -(m_\pi/2)$. The reason for this appears in a transparent way from the equivalent integral formula (A5). In order to explore the domain $\text{Im}k < -(m_\pi/2)$, one has to perform an analytic continuation, the effect of which is discussed in the next section.

B. Zeros of S^{-1} extrapolated to the complex momentum plane

In the vicinity of a pole, located at k_0 , Eq. (2.1) can be written as

$$S(k) = \frac{F(-k)}{F(k)} = \frac{F(-k)}{\alpha(k - \text{Re}k_0 - i\text{Im}k_0)}, \quad (2.3)$$

with

$$\alpha = \left[\frac{dF(k)}{dk} \right]_{k=k_0}.$$

This corresponds to a linear approximation to $S^{-1}(k)$ for k around k_0 , leading to the Breit-Wigner formula. Fits by higher order polynomials provide better approximations. The roots of these polynomials can then be obtained by standard numerical techniques. The extrapolation to complex values of k could be limited by the presence of poles of S^{-1} , which are unknown. However, this does not seem to occur with the resonances we consider.

In order to approximate S^{-1} , we choose the Lagrange interpolating polynomial of degree N over a set of $N+1$ Chebychev mesh points, taken from the real domain $(\text{Re}k_0 + \text{Im}k_0, \text{Re}k_0 - \text{Im}k_0)$. This choice of interpolating points can be shown to provide a nearly optimal approximation.¹² It is then very important to vary N , since knowing only one polynomial, even if it is a good approximation, does not tell us which of its N roots to pick. Varying N , say from 1 to 10, we find that the physically interesting roots are those which converge towards fixed values. For instance, in Ref. 8, the procedure adopted is equivalent to a third degree polynomial approximation. There it is concluded that there are three nearby poles. We think that only one of these is physically significant.

III. RESULTS

We now apply these methods to the Paris $N\bar{N}$ potential. We need to use this potential outside of the physical scattering domain. In searching for resonances, one has to continue to the second sheet in the energy plane. This is quite safe as long as we do not stray too far from the

real axis. The situation is different for the bound states. They lie rather far from the scattering region, where the parameters of the potential are adjusted. Moreover, their energies are sensitive to the energy dependence of the imaginary part of the potential. Thus, predictions concerning bound states might not be reliable, and in this work, we consider only resonances. Since only relatively narrow resonances could give rise to observable effects, we restrict ourselves to the complex momentum domain: $-m_\pi < \text{Im}k < 0$.

Let us first illustrate the effect of the analytic continuation needed for the calculation of the Jost function. In Fig. 1, we plot the coordinates of the pole position for the $^{33}D_2$ partial wave in the complex energy plane, as a function of R , the maximum radius in the integration of the Schrödinger equation. Without analytic continuation, the pole position oscillates and does not converge to any definite value as R increases.

We now consider the case where the imaginary part of the potential is set to zero. Many resonances are found; their complex energies are listed in Table I. Very narrow states, with low as well as high spin, appear. For instance, the widths of the $^{13}P_0$ and $^{33}G_4$ states are 2.4 and 3.2 MeV, respectively. The picture with the complete potential is quite different. These states become wider, many of them now have $\text{Im}k < -m_\pi$. The complex energies and momenta of the poles are also displayed in Table I. With $J < 4$, six states remain, and their width increases with J . The first state, with $J=0$, has $\Gamma=11$ MeV, and the last one, with $J=4$, has $\Gamma=346$ MeV. Most of these widths are comparable to those of ordinary mesons.

When $\text{Im}V_{N\bar{N}}=0$, a pole corresponds to a resonance in the usual sense. That is, it represents a metastable state with a lifetime $\tau=1/\Gamma$. If we increase $\text{Im}V_{N\bar{N}}$ from zero to its final value, it is easy to follow the displacement of the pole in the complex plane. Since it is the same pole which moves to larger Γ , it still seems natural to interpret it as a resonance, with a shorter lifetime than before.

In order to illustrate the dependence of the $N\bar{N}$ spec-

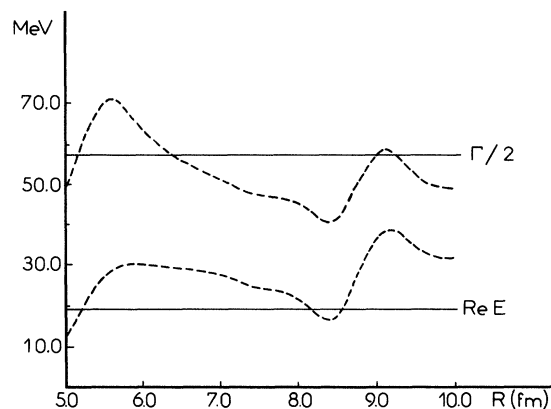


FIG. 1. Behavior of the zero of the Jost function of the $^{33}D_2$ partial wave as a function of R , the distance to which we integrate the Schrödinger equation. The solid and dashed curves are the results with, and without analytic continuation, respectively.

TABLE I. Positions of the S -matrix poles obtained with the real part of the Paris NN potential ($\text{Im } V_{NN} = 0$) and with the complete potential ($\text{Im } V_{NN} \neq 0$).

$2l+12S+1L_J$	$^{13}P_0$	$^{31}P_1$	$^{13}P_1$	$^{11}D_2$	$^{33}D_2$	$^{13}(D-G)_3$	$^{33}(D-G)_3$	$^{33}F_3$	$^{13}(F-H)_4$	$^{33}(F-H)_4$	$^{33}G_4$
$\text{Im } V_{NN} = 0$	$\text{Re } E$ (MeV) 2.4	19	55	71	90	42	105	341	253	96	213
	$\Gamma/2$	1.2	13	13	27	6	17	106	36	0.2	1.7
$\text{Im } V_{NN} \neq 0$	$\text{Re } E$ (MeV) -0.2	-0.5		19	57		132	87	350	317	
	$\Gamma/2$	5.3	31				87		173	102	
	$\text{Re } k$ (fm^{-1}) 0.25	0.61		0.98			1.87		3	2.8	
	$\text{Im } k$	-0.26	-0.62	-0.70			-0.56		-0.7	-0.44	

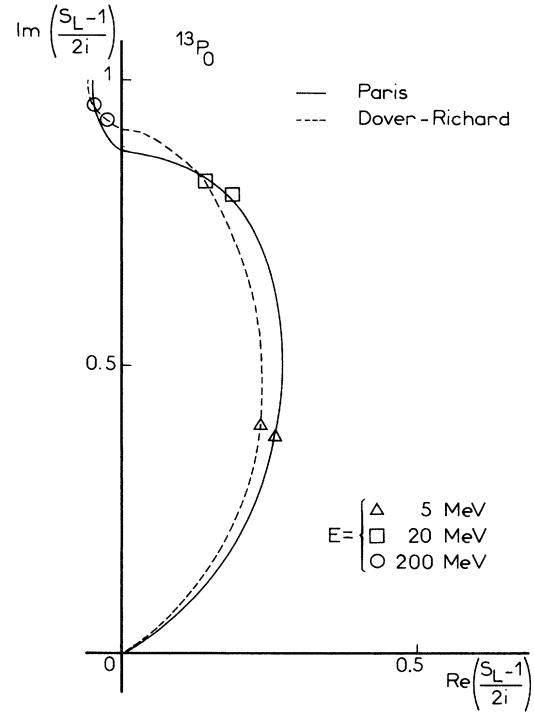


FIG. 2. Argand diagrams of the $^{13}P_0$ partial wave of the Paris potential (solid line), and of the Dover-Richard potential (dashed line).

trum on the properties of the annihilation potential, we also calculate the resonance spectrum using the Dover-Richard potential. In this model, the real part due to meson exchange is the same as in the Paris NN potential, apart from the velocity dependence which is neglected. However, the short and medium range of this real part is modified by the addition of a phenomenological annihilation term. The imaginary part extends to longer distances. The resonances produced by the real part alone

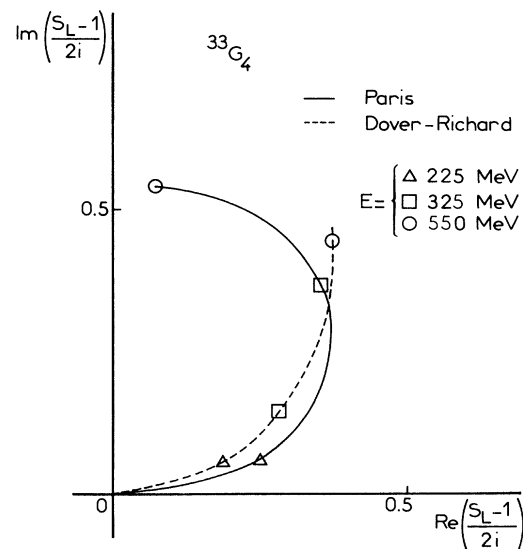


FIG. 3. As in Fig. 2, but for the $^{33}G_4$ wave.

TABLE II. Positions of the S -matrix poles obtained with the real part of the Dover-Richard potential. Using the complete potential, only one state survives, $^{13}P_0$, with $\text{Re}E = -1.9$ MeV and $|\text{Im}E| = \Gamma/2 = 5.1$ MeV.

$2I+12S+1L_J$	$^{13}P_0$	$^{33}P_0$	$^{13}P_1$	$^{13}D_2$	$^{11}F_3$	$^{33}F_3$	$^{13}(F-H)_4$	$^{33}(F-H)_4$
Re E	(MeV) -4.5	66	125	19	288	304	258	254
$\Gamma/2$	0	43	96	0.1	70	143	117	52

are listed in Table II. They are less numerous, and in general, wider than those shown in the first line of Table I. This is due to a very attractive core which favors bound states over resonances. It is interesting to note that here, a $^{13}P_0$ state lies very close to threshold. It is the only state which survives with the complete potential. Its complex energy is $E = -1.9 - i5.1$ MeV, a value close to the Paris potential result, $E = -0.2 - i5.3$ MeV. The other states have on the average $\text{Im}k_0 \approx -2m_\pi$.

Let us now consider the behavior of the phase shift in the vicinity of a pole. In Figs. 2 and 3, we have drawn the Argand diagrams of the $^{13}P_0$ and the $^{33}G_4$ states of Table I. They have the smallest $\text{Im}k_0$ and therefore have the largest chance to influence the scattering. Neither of them shows a loop. Indeed, from Eq. (2.3)

$$\text{Arg}S(k) = 2\delta = -\text{Arg}\alpha + \text{Arg}F(-k) + \tan^{-1} \frac{\text{Im}k_0}{k - \text{Re}k_0}. \quad (3.1)$$

Without annihilation, one has

$$F(-k) = F^*(k) \quad (3.2)$$

and

$$\text{Arg}F(-k) = -\text{Arg}F(k) = \tan^{-1} \frac{\text{Im}k_0}{k - \text{Re}k_0}. \quad (3.3)$$

Then, as k goes through $\text{Re}k_0$, δ increases by an amount close to π . With a strong annihilation, relation (3.2) no longer holds, and we only expect an increase of about $\pi/2$. Do we still have a resonance in the usual sense? We believe the answer is yes. Actually, what is really needed for

a narrow resonance is just a sharp increase of the phase shift.¹¹ Such a sharp increase is present for both the $^{13}P_0$ and $^{33}G_4$ waves, as can be clearly seen in the Argand diagrams of Figs. 2 and 3. This is also true for the $^{13}P_0$ state of the Dover-Richard model, also shown in Fig. 2. In contrast, the $^{33}G_4$ wave in the latter model has no pole in the region $-m_\pi < \text{Im}k < 0$, and the behavior of its Argand diagram is different (Fig. 3).

We also checked that, with our second method, we recover all of the preceding poles. This is illustrated in Table III for the $^{13}P_0$ and the $^{33}G_4$ partial waves of the Paris potential. A pole appears already in the linear approximation. Going to polynomials of fourth or fifth degree, one obtains a value within 10% of the exact one. Higher order is, however, required for a more accurate determination.

IV. CONCLUSION

In the present work, we have studied the spectrum of NN resonances produced by the Paris optical potential. The poles of the S matrix in the complex momentum plane which lie reasonably close to the real axis were found by two different procedures. The masses and widths of these states are listed in Table IV. Two of the six predicted resonances, the $^{13}P_0(1880)$ and $^{33}G_4(2175)$, are expected to give rise to observable effects in NN scattering, even though there is no loop in the Argand diagrams. We find no states which are very narrow ($\Gamma < 10$ MeV, say). The spectrum appears to depend sensitively on the range of the imaginary part of the NN optical potential. For example, with a longer ranged annihilation, the Dover-Richard potential produces a sparser spectrum,

TABLE III. Comparison of the pole positions obtained from approximations of S^{-1} by polynomials of degree N , as a function of N , with the "exact" values obtained by the direct method from the Jost function.

N	$^{13}P_0$		$^{33}G_4$	
	Re k (fm $^{-1}$)	Im k (fm $^{-1}$)	Re k (fm $^{-1}$)	Im k (fm $^{-1}$)
1	0.0083	-0.1531	1.924	-0.1611
2	0.1398	-0.3502	2.409	-0.3915
3	0.2152	-0.2401	2.567	-0.3869
4	0.2456	-0.2993	2.644	-0.3773
5	0.2475	-0.2596	2.690	-0.3715
6	0.2479	-0.2674	2.721	-0.3680
7	0.2492	-0.2624	2.744	-0.3670
8	0.2513	-0.2559	2.762	-0.3667
Exact	0.2507	-0.2565	2.803	-0.4393

TABLE IV. Summary of the properties of the $N\bar{N}$ resonances predicted by the Paris $N\bar{N}$ potential.

$2l+12s+1L_J$	$^{13}P_0$	$^{31}P_1$	$^{33}D_2$	$^{33}F_3$	$^{33}(F-H)_4$	$^{33}G_4$
Mass (MeV)	1880	1880	1899	2008	2202	2175
Width (MeV)	11	62	114	174	346	204
$ \text{Im}k $ (MeV)	57	122	138	111	138	85

with only one resonance ($^{13}P_0$).

To our knowledge, this calculation of the $N\bar{N}$ resonance spectrum is the first one performed with a full optical potential. Earlier calculations^{4,14} employed only real potentials. It is hard to compare the results of those calculations with ours since changes due to the effects of the imaginary potential are important, as we already mentioned. Concerning a comparison with experimental data, if the existence of the so-called S meson¹⁵ with a mass of 1936 MeV and a narrow width ($\Gamma \lesssim 4$ MeV) is confirmed,¹⁶ it cannot be described by the present model. One could, however, conjecturally regard it as a $2q2\bar{q}$ system. It is therefore of great importance that this question be settled by future experiments at LEAR.

ACKNOWLEDGMENTS

We would like to thank C. B. Dover and J. M. Richard for useful discussions. The Division de Physique Théorique de l'Institut de Physique Nucléaire is a Laboratoire Associé au Centre National de la Recherche Scientifique. This work was supported in part by the U.S. D.O.E. contract No. DE-AC02-76ER-13001.

APPENDIX

In the following, we give the formulae used to calculate the Jost function in the domain $-m_\pi < \text{Im}k < 0$. For an angular momentum L , the integral formula for the Jost function $F_L(k)$ is¹¹

$$F_L(k) = 1 + \frac{1}{k} \int_0^\infty dr h_L^+(kr) V(r) \Phi_L(k, r), \quad (\text{A1})$$

where $h_L^+(kr)$ is the Riccati-Hankel function, $V(r)$ is the potential, and $\Phi_L(k, r)$ is the regular solution of the Schrödinger equation. Let R be the maximum value of the radius up to which we integrate. We can split the integral (A1) in two pieces. Defining

$$F_L^R(k) = 1 + \frac{1}{k} \int_0^R dr h_L^+(kr) V(r) \Phi_L(k, r), \quad (\text{A2})$$

we have

$$F_L(k) = F_L^R(k) + \frac{1}{k} \int_R^\infty dr h_L^+(kr) V(r) \Phi_L(k, r). \quad (\text{A3})$$

For R sufficiently large, $R \gg m_\pi^{-1}$, and if $r > R$, $V(r)$ is given by the one-pion-exchange potential $V_{\text{OPE}}(r)$. Neglecting the piece proportional to $h_L^-(kr)$ which is exponentially decreasing since $\text{Im}k < 0$, the asymptotic wave function is¹¹

$$\Phi_L(k, r) \approx -\frac{i}{2} F_L(-k) h_L^+(kr). \quad (\text{A4})$$

Then, from Eq. (A3)

$$F_L(k) = F_L^R(k) - \frac{i}{2} F_L(-k) \int_R^\infty dr [h_L^+(kr)]^2 V_{\text{OPE}}(r). \quad (\text{A5})$$

The computation of $F_L(-k)$ does not cause any trouble since the imaginary part of $-k$ is positive. To give a meaning to the integral in (A5) for $\text{Im}k < -(m_\pi/2)$, one has to perform an analytic continuation. In the following, we provide a simple way to do this. Our results can be expressed in terms of the integrals:

$$I_R^N(k) = \int_R^\infty dr \frac{e^{(2ik - m_\pi)r}}{r^N} = \frac{1}{R^{N-1}} E_N(z), \quad (\text{A6})$$

with

$$z = -(2ik - m_\pi)R, \quad (\text{A7})$$

and where $E_N(z)$ is the exponential integral.¹³ In order to give a meaning to the integral (A6) in the domain $\text{Im}k < -(m_\pi/2)$ we first define

$$g_1(\text{Im}k) = \frac{dI_R^1(k)}{d(-\text{Im}k)} = 2R \frac{e^{-z}}{z}. \quad (\text{A8})$$

Then for any $\text{Im}k < 0$, I_R^1 can be evaluated from the identity

$$I_R^1(k) = \int_0^{-\text{Im}k} g_1(s) ds + I_R^1(\text{Im}k = 0), \quad (\text{A9})$$

where $I_R^1(\text{Im}k = 0)$ can be computed from (A6), and goes to zero exponentially as a function of R . It will therefore be neglected in the following. Now for $N > 1$, from the relation

$$\frac{dI_R^N(k)}{d(-\text{Im}k)} = 2I_R^{N-1}(k), \quad (\text{A10})$$

one gets I_R^N by successive integration. From this, one can deduce the following expression:

$$I_R^N(k) = \int_0^{-\text{Im}k} g_1(s) \frac{[2(-\text{Im}k - s)]^{N-1}}{(N-1)!} ds, \quad (\text{A11})$$

where we have neglected terms which are exponentially small for large R . These expressions are well defined and easy to evaluate numerically. The second term on the right-hand side of Eq. (A5) can now be computed, and one can see from Fig. 1 that its addition to F_L^R results in a converging value for the zeros of $F_L(k)$ as soon as $R \gg m_\pi^{-1}$.

*Also at Faculté des Sciences de Reims, France.

¹T. Kamae, Nucl. Phys. A374, 25 (1982).

²R. Klapisch, An. Fis. 79A, 1 (1983).

³For a review and references see, e.g., H. M. Chan, in *High Energy Physics and Nuclear Structure*, edited by D. F. Measday and A. W. Thomas (North-Holland, Amsterdam, 1980), p. 219.

⁴See, e.g., I. Shapiro, Phys. Rep. 35C, 129 (1978).

⁵J. Weinstein and N. Isgur, Phys. Rev. Lett. 48, 659 (1982); N. A. Törnqvist, *ibid.* 49, 624 (1982).

⁶F. Myhrer and A. Gersten, Nuovo Cimento 37A, 21 (1977).

⁷J. C. H. Van Doremalen, M. Van der Velde, and Yu. A. Simonov, Phys. Lett. 87B, 315 (1979).

⁸Yu. A. Simonov and J. A. Tjon, Nucl. Phys. A319, 429 (1979).

⁹J. Côté, M. Lacombe, B. Loiseau, B. Moussallam, and R. Vinh

Mau, Phys. Rev. Lett. 48, 1319 (1982).

¹⁰C. B. Dover and J. M. Richard, Phys. Rev. C 21, 1466 (1980).

¹¹J. R. Taylor, *Scattering Theory* (Wiley, New York, 1972).

¹²C. de Boor, *A Practical Guide to Splines* (Springer, Berlin, 1978), Vol. 27.

¹³*Handbook of Mathematical Functions*, edited by M. Abramowitz and I. A. Stegun (Dover, New York, 1963).

¹⁴J. M. Richard, M. Lacombe, and R. Vinh Mau, Phys. Lett. 64B, 121 (1976); C. B. Dover and J. M. Richard, Ann. Phys. (N.Y.) 121, 70 (1979).

¹⁵W. Brückner *et al.*, Phys. Lett. 67B, 222 (1977).

¹⁶C. Amsler *et al.*, presented by Th. Walcher at the Workshop on Physics at LEAR, Erice, 1982, CERN Report No. CERN-EP/83-93, 1982; R. Bertini *et al.*, CERN Report No. CERN-EP/82-66, 1982.